2022-03

Heterogeneous weathering of polypropylene in the marine environment

Scott, JW

10.1016/j.scitotenv.2021.152308
Science of The Total Environment
Elsevier BV

"Heterogeneous weathering of polypropylene in the marine environment"

John W Scott [a, *], Andrew Turner [b], Andres F Prada [a], Linduo Zhao [a]

[a] – *The Illinois Sustainable Technology Center, Prairie Research Institute, University of Illinois at Urbana-Champaign, Urbana, IL 61801, USA*

[b] – *School of Geography, Earth and Environmental Sciences, University of Plymouth, Drake Circus, Plymouth PL4 8AA, UK*

[*] Corresponding author: zhewang@illinois.edu (J. Scott)

Keywords: marine plastic; weathering; infrared mapping; carbonyl index; XRF; titanium dioxide

Synopsis: Additives, such as titanium dioxide, utilized in plastics need to be considered when evaluating how these materials degrade in the natural environment.

Abstract Art:

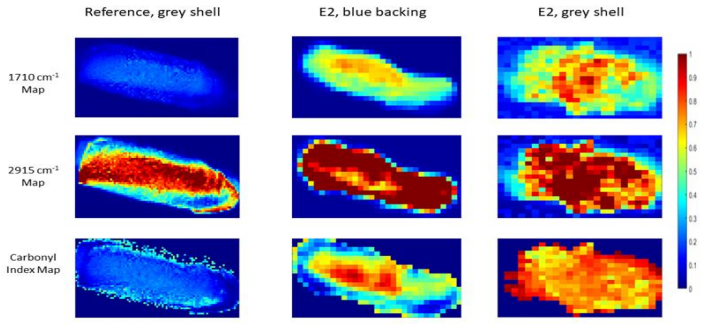

Accepted 7 December 2021

http://dx.doi.org/10.1016/j.scitotenv.2021.152308

Abstract

Polypropylene (PP) inkjet cartridges spilled in the Northwest Atlantic Ocean from a container ship and subsequently retrieved from beaches around Europe and the Azores and a matching reference cartridge that had not been exposed to the environment have been physically and chemically characterized. Compared with the reference, the cartridges retrieved from the marine exhibited considerable cracking-fracturing, discoloration, surface roughness, loss of gloss and staining. Infrared analysis revealed that weathering was highly heterogeneous, with the carbonyl index ranging from < 0.1 to > 0.9 over areas of sub-mm-dimensions. The high degree of weathering was attributed to the presence, quality and distribution of the titanium dioxide pigment, TiO_2. Thus, in the absence of sufficient protection by encapsulation or addition of antioxidants, the ultraviolet light-absorbing pigment promoted the formation of free radicals and photocatalytic oxidation. The results of this study show that consumer plastics containing TiO_2 for coloration or tinting purposes which when not designed for exterior use (in the absence of encapsulation or antioxidants) may experience accelerated weathering in the marine environment and that estimates of plastic persistence should factor in the role of additives that promote photoactivity.

1. Introduction

Because of its toughness and chemical and biological inertness, polypropylene, PP, is one of most widely used plastics. According to the latest data from PlasticsEurope (2020), PP tops the demand for plastics by resin type in Europe, with the greatest share in the food packaging sector. Its extensive contemporary and historical production, coupled with a low density (about 0.9 g cm^{-3} for the pure polymer), also ensure that it is one of the most commonly encountered plastics littering the ocean (Gewert et al., 2017; Massos and Turner, 2017; Andrades et al., 2018).

The dominant mechanism by which PP degrades outdoors is photo-oxidation through the absorption of ultraviolet radiation, resulting in discoloration, loss of mechanical properties, and embrittlement (Bedia et al., 2002). While, in theory, the degradation of polyolefins should be very slow because they do not contain any inherent chromophores that interact with solar radiation, unintentionally introduced contaminants or localized imperfections arising from manufacture may provide a variety of absorbing species that accelerate the process (Yousif and Haddad, 2013). To inhibit the degradation of plastics designed for outdoor use, various additives (e.g., ultraviolet light absorbers and antioxidants) are used, including zinc oxide, ZnO (Brostow et al., 2020) and coated TiO_2 (Jiang et al., 2019). For consumer plastics that are not intended for exterior exposure, however, such protective additives are not required and may be deliberately avoided. Consequently, once introduced into the environment as litter and exposed to conditions they were never designed for, these plastics are predicted to degrade more quickly (Day, 1990).

While the mechanisms of PP photo-degradation under controlled (and accelerated) laboratory conditions have been extensively studied (Rabello and White, 1997; Sobkow and Czaja, 2003; Andrade et al., 2019), it is a complex task to extrapolate the artificially derived results derived to the marine environment for two reasons. Firstly, plastic debris is generated from a variety of manufactured products whose precise original compositions and properties vary considerably (ter Halle et al., 2017). Secondly, external factors, such as day-night temperatures, humidity, biofouling and contamination by corrosive agents are difficult to control or record (Tidjani, 1997).

An alternative way of studying the photo-degradation of plastic litter is to characterize samples retrieved from the environment (Veerasingam et al., 2016; Brignac et al., 2019). While this provides information on the broad nature and impacts of degradation, a quantitative, mechanistic insight relies on knowledge of the age, source and environmental pathways of the samples and having access to the

original, unweathered products as a reference. To this end, we conduct a physical and chemical study of PP Hewlett Packard printer cartridges retrieved from beaches around the North East Atlantic Ocean that had been spilled from a container ship some 1500 km to the east of New York (Turner et al., 2021). Qualitative, quantitative and spatial results arising from the analysis of weathered cartridges are compared with those returned for an identical cartridge that had been housed in a printer and in the dark for its lifespan.

2. Methods

2.1 Samples

Samples used in the study were six, positively buoyant PP Hewlett Packard inkjet cartridges that had been spilled from a container ship in the Atlantic Ocean some 1500 km east of New York in January 2014 and that had subsequently been retrieved by beachcombers from northern Europe and the Azores archipelago. Details of the spillage and cartridges are given in Turner et al. (2021). Briefly, cartridges consist of a grey shell and a backing (black, blue, or pink) that indicated the original color of the ink and contain a hydrophobic foam within the structure that acted as a reservoir for the ink (Figure 1). Cartridges backed with pink or blue are about 70 x 37 x 11 mm in size and weigh about 15 g, while cartridges backed in black are about 70 x 37 x 15 mm and weigh about 20 g. Specifically, cartridges were retrieved from beaches in Cornwall, UK, between December 2015 and June 2016 (E1, E2, E3; black, blue, and pink backings, respectively), northern Norway in June 2017 (E4; blue backing), and the Azores between September 2014 and January 2016 (E5, E6; blue and pink backings, respectively). Dispersion modeling based on drogue tracking data suggests that samples E1 to E3, E4, and E5 and E6 had been suspended in the Atlantic Ocean for at least 16 months, 28 months, and 8 months, respectively (Turner et al., 2021). Subsequently, it was assumed that cartridges resided in the littoral zone, albeit under unknown conditions (sheltered, shaded, buried, trapped in the swash zone), with a maximum total period exposed to the environment of 41 months.

In addition, a reference PP Hewlett Packard inkjet cartridge with a black backing that had not been exposed to the environment was sourced from a printer located at a University of Illinois surplus warehouse. Measurements for each printer cartridge were performed on both the grey shell and colored backing.

2.2 Pyrolysis-gas chromatography

Pyrolysis-gas chromatography mass spectrometry (py-GCMS) was conducted using a CDS Analytical 5200 Series pyroprobe interfaced to a Shimadzu QP2010 SE gas chromatograph. A small (~ 5 mg) sub-sample was cut from the original material and was placed into a quartz capillary tube which was then loaded into the pyroprobe and heated to 600 ^{o}C for 90 s. The temperatures of the GC injection port (split ratio of 100:1) and transfer line were set at 300 ^{o}C. Separation was performed on a capillary column (30 m x 0.25-mm x 0.25 μm film thickness; Restek Rtx-5MS) with helium gas at a flow of 1.0 mL/min. During pyrolysis, the oven was held at 40 ^{o}C for 2 min and then heated to 300 ^{o}C at a rate of 10 ^{o}C/min, and during the course of separation, the mass spectrometer collected data over a mass to charge ion (m/z) range from 35 to 350 Daltons. Blanks were analyzed before and after each sample until an initial baseline was achieved.

2.3 Infrared analysis

Infrared (IR) measurements were performed with a Thermo Scientific Nicolet in10 MX microscope. A small sub-sample (~ 5 mm to 2 mm) was cut from original material and was mounted on a gold-coated reflective slide. Spectra were acquired in both attenuated total reflection (ATR) and reflective mapping modes. In ATR mode, six spots were randomly selected across the sample surface and were obtained over a wavelength range of 675-4000 cm^{-1} at a resolution of 4 cm^{-1} and at 32 scans per spot. Infrared mapping was performed in reflectance mode over the entire surface of the offcut and obtained over a range of wavelengths from 675-4000 cm^{-1} at a resolution of 8 cm^{-1} and at 8 scans per spot. The number of points sampled on each of the materials ranged from approximately 1000 to 4000, depending on the precise size of the offcut. All spectra were background subtracted.

Carbonyl index (CI) is a commonly used approach to evaluate the degree of weathering in polyolefins (Almond et al. 2020, Andrady, Pegram, and Tropsha 1993, Rodrigues et al. 2018). For PP, the CI is calculated using the peak intensity observed in the region of carbonyls (I ~ 1700 cm^{-1}) normalized to the peak intensity of methylene absorption (I ~ 2900 cm^{-1}), since the latter is not influenced by photo-degradation (Butylina, Martikka, and Kärki 2015):

$$\mathrm{CI} = \frac{I_{1710}}{I_{2915}} \qquad \text{(eq. 1)}$$

Custom MATLAB scripts were developed to extract data from the infrared analysis, estimate the CI, and plot distributional maps and histograms.

2.4 SEM and XRF analyses

The offcuts used for the IR measurements were subsequently transferred onto a conductive and adhesive carbon tape mounted on an aluminum SEM sample holder. Morphological characterization was performed using a Field-Emission Environmental Scanning Electron Microscope (FEI-ESEM, Quanta FEG 450). To avoid the sample preparation that may result in small morphological changes, all offcuts were directly imaged in the low vacuum mode at 1.0 Torr without metal coating. SEM images were collected at a working distance of 7-13 mm, with an accelerating voltage of 7-10 kV and a spot size of 40-50 μm.

Elemental analysis of the polymer surfaces of the cartridge components was performed in duplicate or triplicate with a Rigaku NEX CG Energy Dispersive X-Ray Fluorescence (ED-XRF) spectrometer housed at the Illinois State Geological Survey. The instrument specifications included a 50 W Pd-anode end window X-ray tube, four secondary targets (RX9, Cu, Mo, and Al), a 20 mm diaphragm, and a high-performance silicon drift detector (SDD). Measuring times were 100 seconds (RX9, Cu, and Mo) and 200 seconds (Al) and counts were converted to percentage concentrations by weight using QuantEZ® software.

3. Results and Discussion

3.1. Sample characteristics

Examples of the cartridges considered in the study are illustrated in Figure 1. Compared with the reference cartridge obtained directly from a printer and that had not been exposed to the environment, cartridges lost in the Atlantic Ocean for up to 41 months and retrieved from north Atlantic beaches (E1 to E6) display cracking, scratching, surface roughness and deformation, with the grey shells exhibiting some discoloration, loss of gloss, and extensive surface ablation or chalking (evident when handling or manipulating samples and from fragments of plastic embedded in exposed foam).

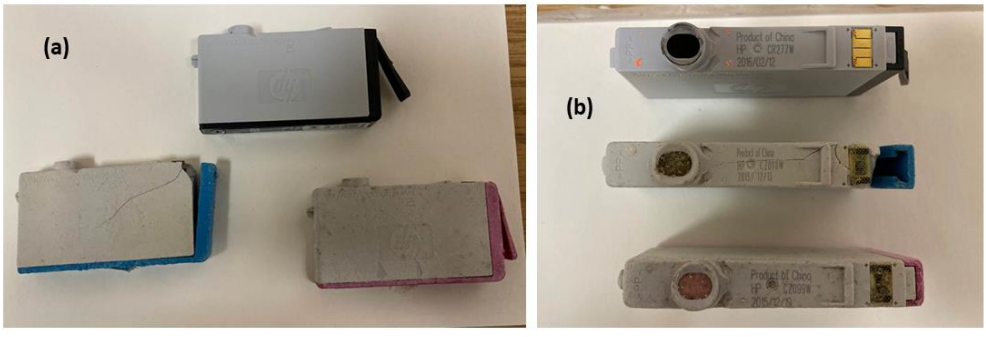

Figure 1: (a) Face and (b) side views of the reference cartridge (black backing) and samples E2 (blue) and E3 (pink). Note that, for scale, cartridge length is about 70 mm and cartridge width is 11 to 15 mm.

Figure 2 presents py-GCMS chromatograms for the black backing associated with the reference print cartridge and the black backing of a naturally weathered cartridge, E1. The predominant pyrolysis products observed were 2,4-dimethyl-1-heptene, PP tetramers (2,4,6-trimethyl-1-nonenes), and PP pentamers (2,4,6,8-tetramethyl-1-undecanes). These compounds are known decomposition products observed during pyrolysis of PP and the average spectra from the py-GCMS results agree well with literature references for the same material (Tsuge, Ohtani, and Watanabe 2011, Wampler 2006). Overall, py-GCMS data for all samples analyzed were very similar, even though cartridges exposed to the marine environment were drastically weathered (and as observed visually and by infrared analysis). This demonstrates the utility of py-GCMS for accurate identification of plastics found in the environment, regardless of their state of degradation.

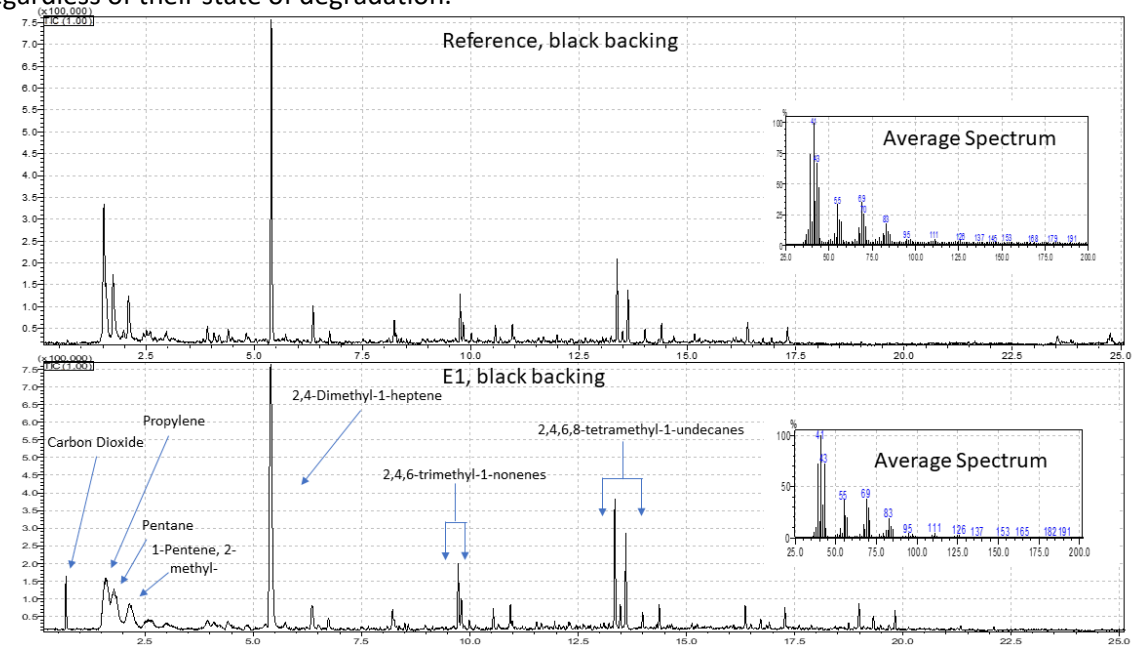

Figure 2: Chromatograms from py-GCMS analysis of the black backings of the reference cartridge and sample E1.

All PP components exposed to the environment in this study produced a carbon dioxide peak during pyrolysis. Likewise, in a previous study that investigated the aging of PP after exposure to

ultraviolet light, carbon dioxide was identified in samples analyzed by py-GCMS after only 30 days (Ainali, Bikiaris, and Lambropoulou 2021). Although this suggests that the presence of a carbon dioxide peak may provide an alternative means of assessing the state of degradation of PP, its presence in the grey shell of the reference cartridge means that further investigations would be required to explore this possibility.

Two examples of ATR-IR spectra (for six spots on the grey shells of the reference cartridge and sample E4) are shown in Figure 3. All spectra contained the characteristic signals for PP in the 2800 cm^{-1} to 3000 cm^{-1} regions, and at 1460 cm^{-1} and 1378 cm^{-1} wavenumbers. These vibrational absorptions are due to the C-H bonds (2800 cm^{-1} to 3000 cm^{-1}), the methylene CH_2 groups (1460 cm^{-1}), and methylene CH_3 groups (1378 cm^{-1}) in the polymer structure (Abu‐Isa 1970, Rjeb et al. 2000). All samples exposed to the environment (and both grey and colored components), had an additional broad peak located in the 3000 cm^{-1} to 3680 cm^{-1} region and another in the 1650 cm^{-1} to 1850 cm^{-1} region due to absorption by oxidation products (hydroxyl groups and aldehydes and ketones, respectively; (Barbeş, Rădulescu, and Stihi 2014, Manfredi, Barberis, and Marengo 2017). However, since the ATR-IR technique requires contact with the surface of the material, the degree of degradation can be highly dependent on the surface sites selected for analysis. This is evident in the high degree of variability observed in the absorption intensities for oxidation products at six different locations of the grey shell of the beached cartridge (E4; Figure 3). It is also interesting to note that, despite this variability, the intensities for the methylene groups associated with the original polymer were rather consistent. This further demonstrates that methylene group absorptions are not influenced by degradation and are well justified to be used as a normalization factor in the CI calculation.

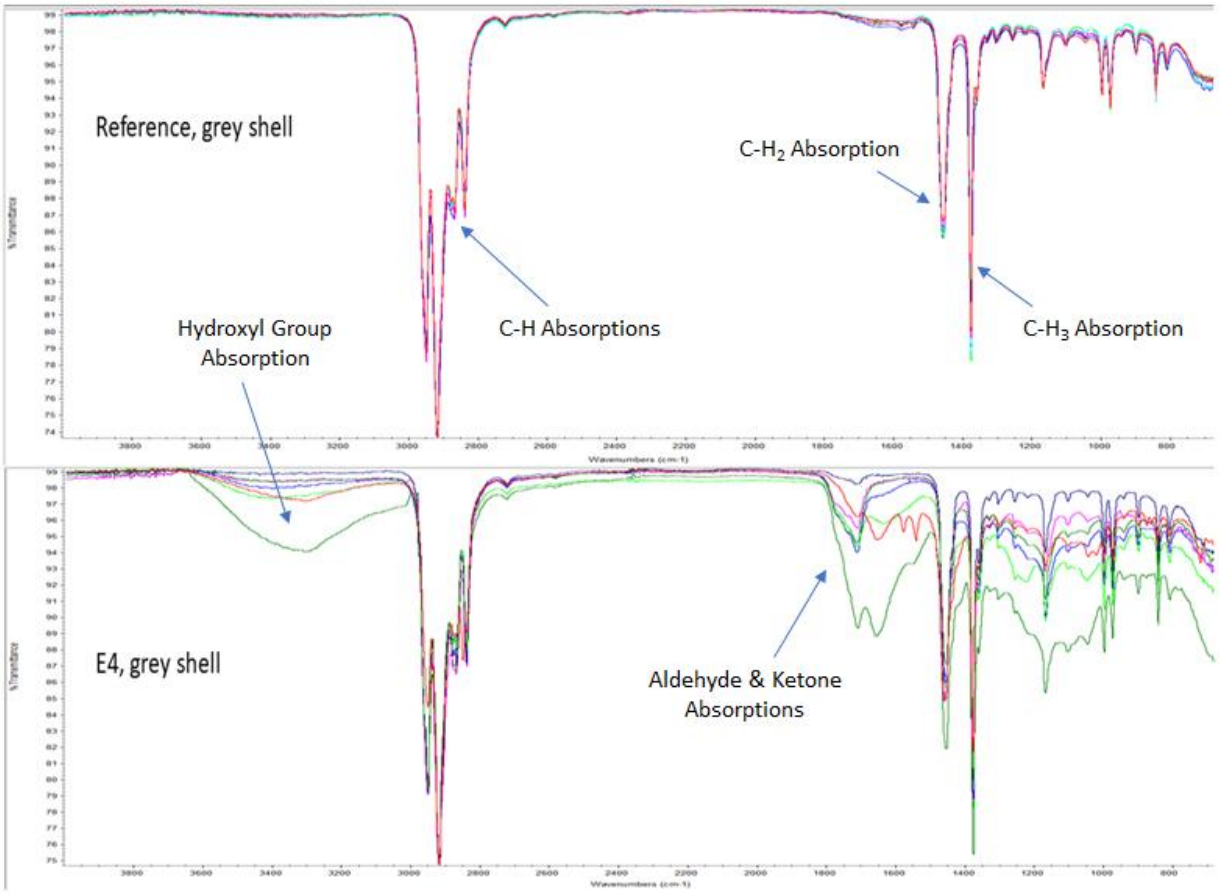

Figure 3: Overlays of six ATR-IR spectra for the grey shells of the reference cartridge and sample E4.

3.2. Surface mapping by Reflectance-IR and SEM

Figure 4 shows examples of the high-resolution infrared data obtained from surface mapping of the mm-sized offcuts performed in reflectance mode in order to obtain spatial information on PP degradation in the samples. Specifically, the top row of images shows the data extracted at 1710 cm^{-1} for the grey shell of the reference cartridge and the grey shell and blue backing of sample E2, the middle row shows the data extracted at 2915 cm^{-1} for these samples, and the bottom row presents the resulting CI distributions. The drastic differences in intensities over the entire surface of the sample exposed to the environment may be partly attributed to differences in surface topography. However, the estimation of CI (as an intensity ratio) corrects for this effect and provides a better indicator of the spatial degradation of the plastic. Thus, degradation of the PP exposed to the marine environment is highly heterogeneous over sub-mm dimensions and appears to be greater in the grey shells than in the

colored backings. The CI mapping of the reference cartridge reveals a low content of carbonyl functional group throughout the imaging area, suggesting low or no weathering. As expected, the red areas indicate a high content of carbonyl functional groups and were observed in the CI mapping of sample E2, due to environmental exposure. Interestingly, although exposed to the same environmental conditions for the same period, the grey shell of sample E2 exhibits a larger red area in the CI map than blue backing, suggesting a higher content of carbonyl functional group as well as a stronger degradation.

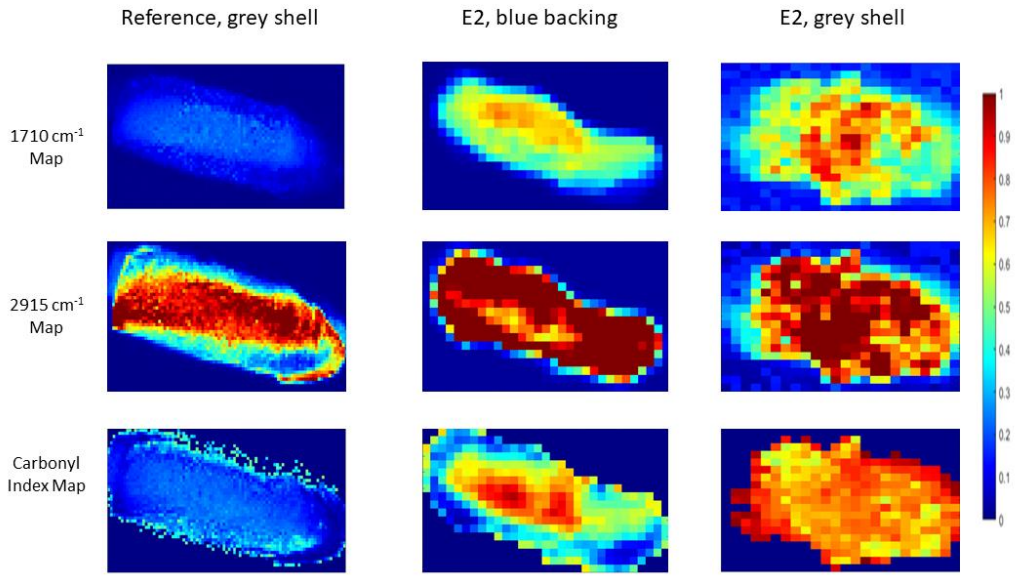

Figure 4: Reflectance-IR maps (at 1710 cm^{-1} and 2915 cm^{-1}) and carbonyl indices for selected cartridges.

The plastic offcuts analyzed by IR were subsequently imaged by SEM to compare their surface morphologies. Figures 5A to 5C show the three offcuts mapped by ATR-IR in Figure 4 at low magnification (X40-70), with the two areas selected based on the carbonyl index map for imaging at higher magnification. For the grey shell from the reference cartridge, both areas of low CI are representative of the entire surface which exhibits little degradation, and SEM images at high magnification (Figures 5D & 5G) show a smooth and even surface. For the blue backing of sample E2,

two areas were selected which have distinct CIs according to Figure 4. The magnified SEM image of the top area and of high CI revealed an eroded surface with numerous pits, grooves, and cracks (Figure 5E), while the bottom area of lower CI shows a comparatively smooth surface and adhering particles which are presumably precipitated minerals (Figure 5G). Both selected areas of the grey shell of sample E2 exhibited high CIs and magnified SEM images reveal strongly eroded surfaces characterized by numerous pits, grooves, and microcracks (Figures 5F & 5I).

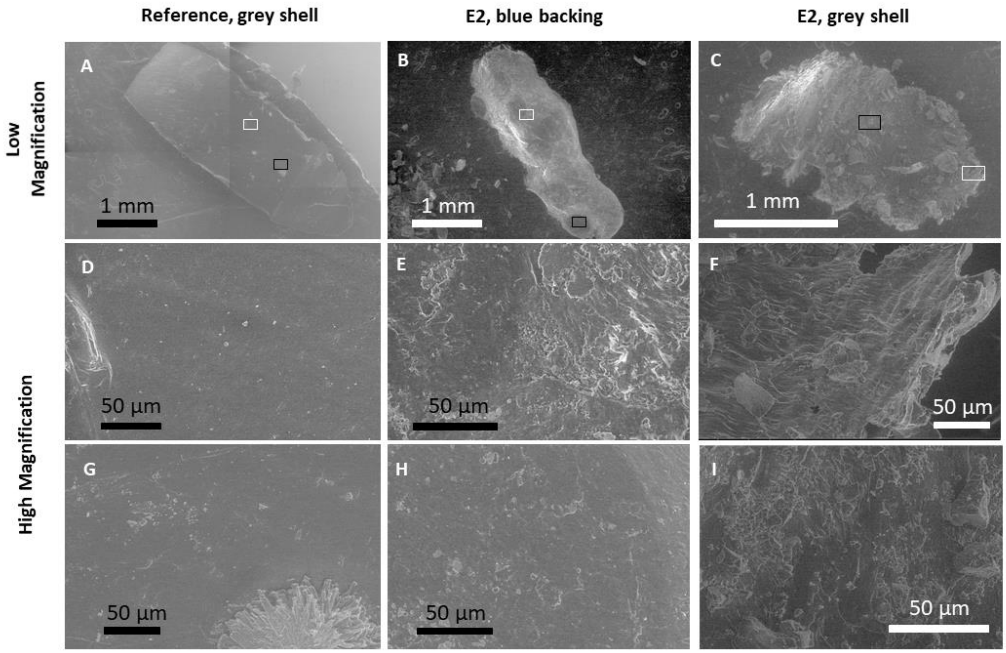

Figure 5: Low and high magnification SEM images for the cartridges selected in Figure 4. The white and black boxes in the upper, low magnification images show the locations for the corresponding high magnification images immediately below and at the bottom, respectively.

The CI data arising from all plastic offcuts analyzed were used to generate histograms that illustrate the magnitude of the index, or the extent of weathering, by surface areal coverage (Figure 6). Some degradation occurred to the reference cartridge, and in particular to the grey casing, but cartridges exposed to the environment exhibit (mainly) Gaussian distributions that are shifted to higher CI and with peak percent areas centered around 0.4 to 0.7 for colored backings (except E1 which showed a gradual increase in area with CI) and around 0.5 to 0.8 for grey shells.

Despite different timescales spent in the environment and distances carried by ocean current, there are no clear or systematic differences in the patterns of weathering among the cartridges lost from the spillage. Rather, degradation appears to be highly heterogeneous both within and between samples and, overall, takes place relatively rapidly, effects that we attribute to the presence and nature of TiO_2 particles in the plastic matrix and as described below.

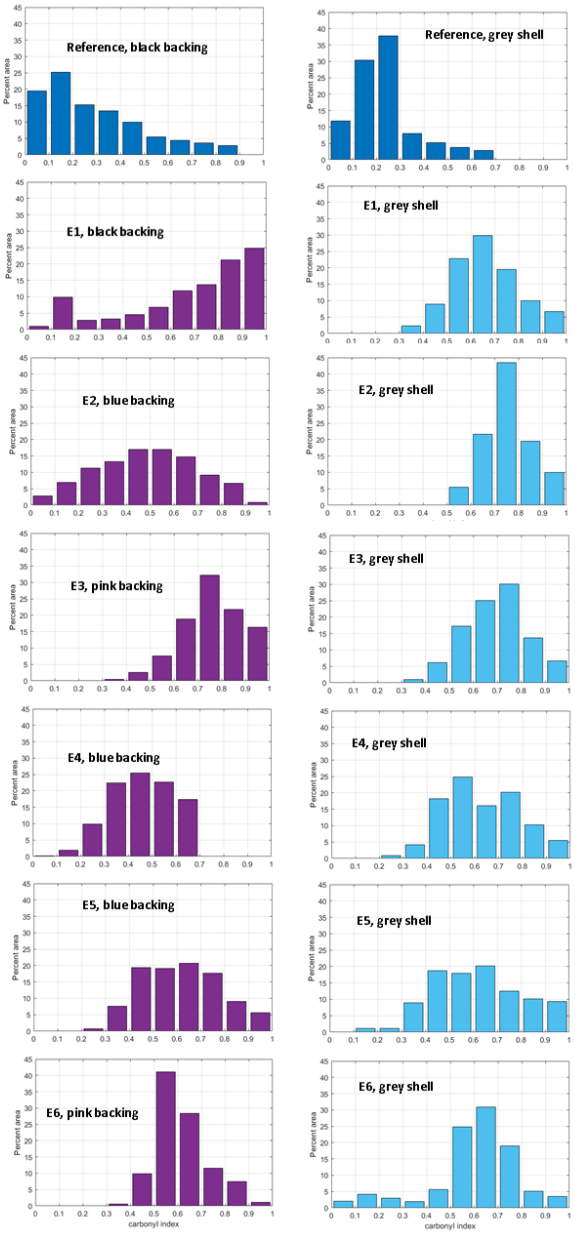

Figure 6. Carbonyl index histograms for all cartridges analyzed by reflectance IR.

3.3 The role of TiO_2 in polypropylene degradation

Titanium dioxide is frequently added to plastics and paints as an inert and non-toxic white pigment and ultraviolet light absorber. Despite its protective properties, however, radiation absorbed can produce free radicals that cause photo-oxidation and photocatalytic degradation (Day, 1990). In outdoor plastics, this effect may be inhibited by incorporating other additives (e.g., antioxidants and light stabilizers) into the matrix or coating the exterior of pigment particles with an impervious oxide (commonly silica; Kemp and McIntyre, 2000). For most consumer products, including packaging, there is no requirement for good exterior weatherability, and, in light of the pervasiveness of plastic waste, efforts are often made to encourage biodegradation and photodegradation. It is likely that the print cartridges in the present study have little inherent protection from weathering as they were never designed for exterior use and it is hypothesized that their weathering in the marine environment is accelerated by the presence of uncoated titanium dioxide pigments.

Unfortunately, the beam area and detector window of the ED-XRF do not allow for a spatial resolution of elemental measurements better than a few mm. Nevertheless, the results arising from the broader analysis of the cartridges, shown in Table 1, reveal that Ti was most abundant (p = 0.0003 according to a paired t-test) and more consistent in concentration (0.87$\pm$0.07 %) in the grey shells of the cartridges, where whitening and opacity were desired, than in the colored backings (0.29$\pm$0.23 %), where TiO_2 may have been used for tinting purposes (Day, 1990). In contrast, and in all but one case (sample E1), concentrations of Si, a proxy for hydrated silica, were considerably higher in the backing than in the corresponding shell (and, overall, p = 0.013 according to a paired t-test). (Note that metals of other common pigments used in PP, Ba, Fe and Zn, were always < 0.015% by weight).

Consistent with the inferences from the CI results and SEM images above and the ready chalking observed (resulting from the degradation of the polymer as TiO_2 particles become progressively exposed; Kemp and McIntyre, 2000), the shells of the cartridges appear to have a greater abundance of ultraviolet-absorbing particles of lower protection than the backings, resulting in a greater propensity for photocatalytic degradation. Luo et al. (2020) recently showed that low density polyethylene microplastics (< 500 μm in diameter) pigmented with 60% TiO_2 (as rutile) exhibited a reduction in CI after artificial aging for several weeks at 60^{o}C and an irradiance of 1200 W m^{-2}. When exposed to freshwater, aged microplastics also released greater quantities of TiO_2 pigment particles and particles of larger diameter than those released from unaged plastic.

Table 1: Mean titanium and silicon contents of the shells and backings of the cartridges determined by ED-XRF.

cartridge	component	Ti, %	Si, %
reference	shell	0.76	0.013
	black backing	0.56	0.16
E1	shell	0.78	0.39
	black backing	0.003	0.38
E2	shell	0.95	0.054
	blue backing	0.44	0.15
E3	shell	0.88	0.10
	pink backing	0.10	0.18
E4	shell	0.90	0.056
	blue backing	0.45	0.11
E5	shell	0.92	0.082
	blue backing	0.43	0.37
E6	shell	0.92	0.055
	pink backing	0.077	0.13

3.4 General implications

This study has demonstrated the utility of infrared mapping for examining the spatial distribution of weathering of environmental plastics. It indicates that measurements should not rely on single-point analysis as conclusions may be influenced by the surface site selected for investigation. Specifically, by comparing and matching, unweathered and naturally weathered plastic inkjet cartridges, this study has shown that PP photodegrades heterogeneously, with the CI varying from < 0.1 to > 0.9 over sub-mm dimensions in some cases. Different components of the same product and constructed of the same polymer also degrade at different rates.

We attribute our observations to the presence and heterogeneous dispersion of TiO_2 pigment particles, added to the cartridges for color, opacity, and tinting. Critically, the quality of the pigments designed for indoor consumer goods, coupled with the absence of other protective additives, allows free radicals to form and photocatalytic oxidation to proceed when exposed to the external environment. Because of the ubiquity of TiO_2 in plastics used in all sectors (some sources indicate it is the most widely used pigment in plastics; Kemp and McIntyre, 2000) and its ready detection in plastics lost to the environment (Fries et al., 2013; Turner and Solman, 2016), we suspect that the processes identified in the present study might be more generally applicable to marine plastic litter derived from the consumer

waste stream. Particularly pigmented polyolefins are likely to be susceptible to accelerated weathering because their positive buoyancy ensures that they are exposed to sunlight throughout their residence times suspended in the ocean.

Based on the type, molecular weight and crystallinity of the polymer, the presence and degradability of fillers, and the size, shape, and thickness of the material it has been predicted that some plastics may persist for several hundred to a few thousand years in the marine environment (Chamas et al., 2020). To this end, the physical characteristics of the inkjet cartridges alone suggest an environmental lifespan towards the latter estimate, but clearly this is inconsistent with the significant weathering and chalking (loss of mass) observed within about 40 months of exposure. More accurate predictions of environmental persistence and the propensity for macro- and mesoplastics to form microplastics therefore require a better understanding of the roles of intentionally added pigments that either accelerate or inhibit photo-oxidation. Also required is an assessment of any environmental impacts associated with the mobilization of TiO_2 micro- and nanoparticles mobilized when plastics degrade (Fries et al., 2013; Roma et al., 2020).

Declaration of competing interest

The authors declare no conflict of interest.

Acknowledgments

We thank Tracey Williams, Lost at Sea Project, for coordinating the collection of the cartridges used in the study.

References

Abu‐Isa, I., 1970. "Thermal degradation of thin films of isotactic polypropylene and polypropylene with ketonic additives." *Journal of Polymer Science Part A‐1: Polymer Chemistry* 8 (4):961-972.

Ainali, N.M., Bikiaris, D.N., Lambropoulou, D.A., 2021. "Aging effects on low-and high-density polyethylene, polypropylene and polystyrene under UV irradiation: an insight into decomposition mechanism by Py-GC/MS for microplastic analysis." *Journal of Analytical and Applied Pyrolysis*:105207.

Almond, J., Sugumaar, P., Wenzel, M.N., Hill, G., Wallis, C., 2020. "Determination of the carbonyl index of polyethylene and polypropylene using specified area under band methodology with ATR-FTIR spectroscopy." *e-Polymers* 20 (1):369-381.

Andrade, J., Fernandez-Gonzalez, V., Lopez-Mahia, P., Muniategui, S., 2019. A low-cost system to simulate environmental microplastic weathering. Marine Pollution Bulletin 149, 110663.

Andrades, R., Santos, R.G., Joyeux, J.C., Chelazzi, D., Cincinelli, A., Giarrizzo, T., 2018. Marine debris in Trindade Island, a remote island of the South Atlantic. Marine Pollution Bulletin 137, 180-184.

Andrady, A.L., Pegram, J.E., Tropsha, Y., 1993. "Changes in carbonyl index and average molecular weight on embrittlement of enhanced-photodegradable polyethylenes." *Journal of environmental polymer degradation* 1 (3):171-179.

Barbeş, L., Rădulescu, C., Stihi, C., 2014. "ATR-FTIR spectrometry characterisation of polymeric materials." *Romanian Reports in Physics* 66 (3):765-777.

Bedia, E.L., Paglicawan, M.A., Bernas, C.V., Bernardo, S.T., Tosaka, M., Kohjiya, S., 2002. Naturalweatehring of polypropylene in a tropical zone. Jounral of Applied Polymer Science 87, 931-938.

Brignac, K.C., Jung, M.R., King, C., Royer, S.J., Bickley, L., Lamson, M.R., Potemra, J.T., Lynch, J.M., 2019. Marine debris polymers on main Hawaiian Island beaches, sea surface, and seafloor. Environmental Science and Technology 53, 12218-12226.

Brostow, W., Lu, X., Gencel, O., Osmanson, A.T., 2020. Effects of UV Stabilizers on Polypropylene Outdoors. Materials 13(7), 1626.

Butylina, S., Martikka, O., Kärki, T., 2015. "Weathering properties of coextruded polypropylene-based composites containing inorganic pigments." *Polymer Degradation and Stability* 120:10-16.

Chamas, A., Moon, H., Zheng, J., Qiu, Y., Tabassum, T., Jang, J.H., Abu-Omar, M., Scott, S.L., Suh, S., 2020. Degradation of plastics in the environment. Sustainable Chemistry & Engineering 8, 3494-3511.

Day, R.E., 1990. "The role of titanium dioxide pigments in the degradation and stabilisation of polymers in the plastics industry." *Polymer Degradation and Stability* 29 (1):73-92.

Fries, E., Dekiff, J.H., Willmeyer, J., Nuelle, M.T., Ebert, M., Remy, D., 2013. Identification of polymer types and additives in marine microplastic particles using pyrolysis-GC/MS and scanning electron microscopy. Environmental Science Processes and Impacts 15, 1949.

Gewert, B., Ogonowski, M., Barth, A., MacLeod, M., 2017. Abundance and composition of near surface microplastics and plastic debris in the Stockholm Archipelago, Baltic Sea. Marine Pollution Bulletin 120, 292-302.

Jiang, T., Wang, S., Zhang, J., 2019. "Enhanced UV resistance of solar cooling high density polyethylene/titanium dioxide composites for long outdoor life via synergy effect of UV absorber and antioxidant." *Journal of Vinyl and Additive Technology* 25 (3):303-309.

Kemp, T.J., McIntyre, R.A., 2000. Mechanism of action of titanium dioxide pigment in the photodegradation of poly(vinyl chloride) and other polymers. Progress in Reaction Kinetics and Mechanisms 26, 337-374.

Luo, H., Xiang, Y., Li, Y., Zhao, Y., Pan, X., 2020. Weathering alters surface characteristic of TiO_2-pigmented microplastics and particle size distribution of TiO_2 released into water. Science of the Total Environment 729, 139083.

Manfredi, M., Barberis, E., Marengo, E., 2017. "Prediction and classification of the degradation state of plastic materials used in modern and contemporary art." *Applied Physics A* 123 (1):1-11.

PlasticsEurope, 2020. Plastics - the facts 2020. an analysis of European plastics production, demand and waste data. https://www.plasticseurope.org/application/files/3416/2270/7211/Plastics_the_facts-WEB-2020_versionJun21_final.pdf

Rabello, M.S., White, J.R., 1997. The role of physical structure and morphology in the photodegradation behaviour of polypropylene. Polymer Degradation and Stability 56, 55-73.

Rjeb, A., Tajounte, L., Chafik El Idrissi, M., Letarte, S., Adnot, A., Roy, D., Claire, Y., Périchaud, A., Kaloustian, J., 2000. "IR spectroscopy study of polypropylene natural aging." *Journal of applied polymer science* 77 (8):1742-1748.

Rodrigues, M.O., Abrantes, N., Gonçalves, FJM., Nogueira, H., Marques, JC, Gonçalves, A.M.M., 2018. "Spatial and temporal distribution of microplastics in water and sediments of a freshwater system (Antuã River, Portugal)." *Science of the total environment* 633:1549-1559.

Roma, J., Matos, A.R., Vinagre, C., Duarte, B., 2020. Engineered metal nanoparticles in the marine environment: A review of the effects on marine fauna. Marine Environmental Research 161, 10.1016/j.marenveres.2020.105110.

Sobkow, D., Czaja, K., 2003. Influence of accelerated ageing conditions on the process of polyolefines degradation. Polimery 48, 627-632.

ter Halle, A., Ladirat, L., Martignac, M., Mingotaud, A.F., Boyron, O., Perez, E., 2017. To what extent are microplastics from the open ocean weathered? Environmental Pollution 227, 167-174.

Tidjani, A., 1997. Photooxidation of polypropylene under natural and accelerated weathering conditions. Journal of Applied Polymer Science 634, 2497-2503.

Tsuge, S, Hajima Ohtani, H., Watanabe, C., 2011. *Pyrolysis-GC/MS data book of synthetic polymers: pyrograms, thermograms and MS of pyrolyzates*: Elsevier.

Turner, A., Solman, K.R., 2016. Analysis of the elemental composition of marine litter by field-portable-XRF. Talanta 159, 262-271.

Turner, A., Williams, T., Pitchford, T., 2021. Transport, weathering and pollution of plastic from container losses at sea: Observations from a spillage of inkjet cartridges in the North Atlantic Ocean. Environmental Pollution 284, 117131.

Veerasingam, S., Saha, M., Suneel, V., Vethamony, P., Rodrigues, A.C., Bhattacharyya, S., Naik, B.G., 2016. Characteristics, seasonal distribution and surface degradation features of microplastic pellets along the Goa coast, India. Chemosphere 159, 496-505.

Wampler, T.P., 2006. *Applied pyrolysis handbook*: CRC press.

Yousif, E., Haddad, R., 2013. Photodegradation and photostabilization of polymers, especially polystyrene: a review. Springerplus 2, 398.